The Production of Positive Mesons by Photons*

J. STEINBERGER
Columbia University, New York, New York

AND

A. S. BISHOP
University of Zurich, Zurich, Switzerland

(Received October 26, 1951)

Experimental results are presented on the production of positive mesons in hydrogen and carbon, as a function of meson angle and energy. The principal results are as follows: The angular distribution in the case of hydrogen is rather flat in the region 45°–135° in the laboratory system, slightly peaked near 90°. This demonstrates that the pion is not a scalar. The excitation function at 90° rises approximately linearly to a plateau which starts at photon energies of about 260 Mev. This rise is slower than expected on the basis of a phase space argument. The total cross section for 255-Mev photons in hydrogen is $1.9\pm0.3\times10^{-28}$ cm^2. The cross sections in carbon are lower, per proton, by a factor of approximately three. With respect to hydrogen, the meson energy distribution is shifted to lower energies and the angular distribution is shifted to the backward angles.

I. INTRODUCTION

THE construction of x-ray machines of sufficient energy has made it possible to study the process of meson production by photons. Photomesons were first found by McMillan, Peterson, and White.[1] We report here the results of more detailed experiments, especially on the process $p+h\nu\rightarrow n+\pi^+$. The experiments were carried out in the hope that this process, which seems particularly suited to analysis because of its simplicity, may shed some light on the interaction of mesons with nucleons.

The following data are presented: (1) The energy dependence of the mesons produced at 90° to the beam direction, both for carbon and hydrogen targets and the excitation function for the production of positive mesons on hydrogen. (2) The angular dependence of the production cross section. (3) The total cross section for meson production by 255-Mev photons on hydrogen.

The experiments have been in part reported.[2]

II. X-RAY CHARACTERISTICS

The x-rays employed in these experiments are produced in the Berkeley synchrotron. This machine accelerates electrons to an energy of 325 Mev and then permits them to strike a target of 0.020-in. platinum. About 15 percent of the electron energy is converted to x-rays with an angular spread of 1° half-width, and characteristic bremsstrahlung spectrum. Figure 1 shows the spectrum, as calculated and corrected for the effects of finite target thickness, and variation of the magnetic field during expulsion of the beam. Cloud-chamber measurements of the spectrum by Powell, Hartsough, and Hill[3] are in agreement with the theoretical results. The expulsion time is purposely made long in order to minimize the accidental coincidence rate in counting experiments.[4] The machine is pulsed 5 times/sec, each beam pulse lasting approximately 0.003 sec. The duty cycle is therefore ~0.015 (Fig. 2).

The beam is monitored by a self-cycling ionization chamber, calibrated by Blocker and Kenney against the ionization chamber used in an absolute measurement of the beam intensity.[5] Their calibration, which has an uncertainty estimated to be less than 10 percent, has been used in all determinations of absolute cross section.

III. KINEMATICS

We study the reaction $p+h\nu\rightarrow n+\pi^+$ for free protons as well as those bound in carbon nuclei. In the case of the reaction with free protons, there are only two

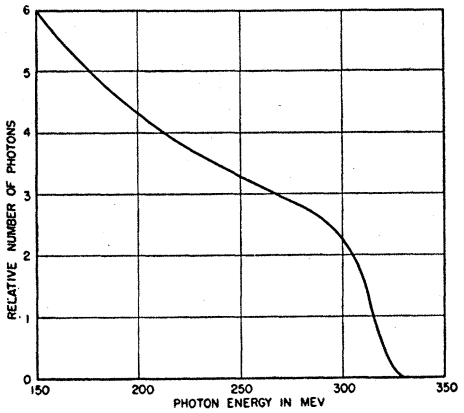

FIG. 1. Calculated x-ray spectrum, corrected for finite target thickness and variation of magnetic field during the expulsion period.

* Research supported by the AEC.

[1] McMillan, Peterson, and White, Science **110**, 579 (1949).

[2] J. Steinberger and A. S. Bishop, Phys. Rev. **78**, 493 (1950), **78**, 494 (1950); Bishop, Steinberger, and Cook, Phys. Rev. **80**, 291 (1950).

[3] Powell, Hartsough, and Hill, Phys. Rev. **81**, 213 (1951).

[4] This is accomplished, on the suggestion of E. M. McMillan, by shaping the envelope of the rf accelerating voltage. G. Gauer and C. Nunan, University of California Radiation Laboratory Report No. 714 (1950).

[5] Blocker, Kenney, and Panofsky, Phys. Rev. **79**, 419 (1950).

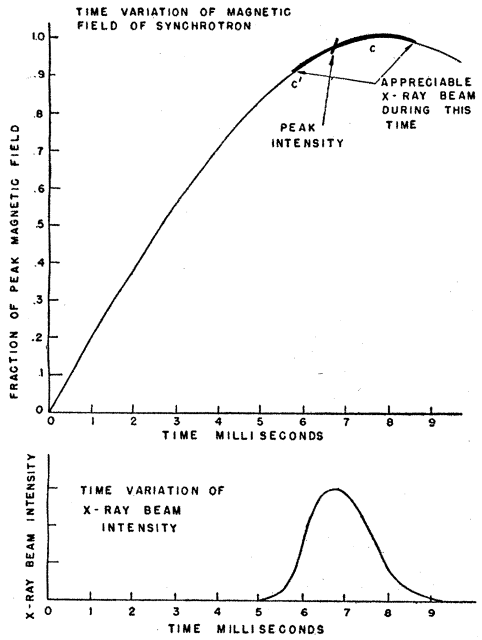

FIG. 2. Duty cycle of the synchrotron.

outgoing particles, and, by the conservation laws, a knowledge of the meson energy and production angle suffice to determine the reaction kinematics, and in particular, the energy of the responsible light quantum.

$$h\nu=\left(E-\frac{\kappa^2}{2M}\right)\Big/\left(1-\frac{E}{M}+\frac{2k\cos\theta}{M}\right), \qquad (1)$$

neglecting the n-p mass difference. Here $h\nu$=photon energy; k, E=meson momentum, energy; κ=meson rest energy; M=proton rest energy; $\hbar=c=1$. This fact makes it possible to measure the proton cross sections as a function of γ-ray energy, despite the continuous nature of the x-ray spectrum. (See Fig. 3.)

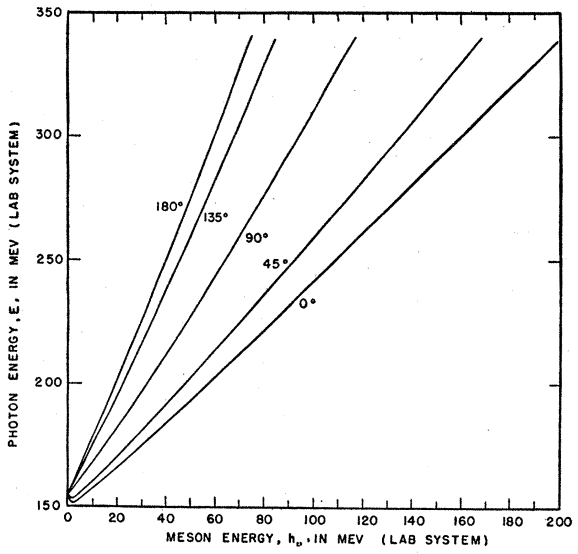

FIG. 3. Photon energy as a function of meson energy and emission angle in the laboratory system, for the reaction,

$$p+h\nu\rightarrow\pi^++n.$$

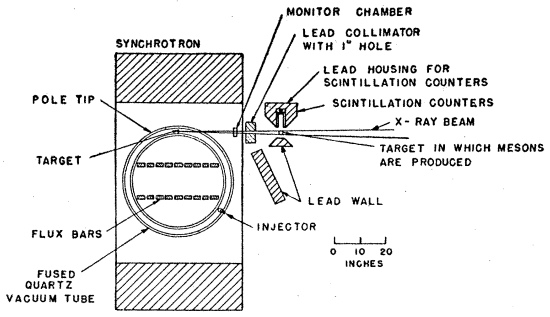

FIG. 4. Arrangement of apparatus.

IV. EXPERIMENTAL ARRANGEMENT

a. General

The x-ray beam is collimated to a diameter of 1 in. at a distance of five feet from the internal target. It is then allowed to strike a target of the material whose meson production cross section is being measured. (See Figs. 4 and 5.) The meson detector consists of three crystal counters, anthracene or stilbene, each approximately $1\frac{3}{4}$ in.$\times 1\frac{3}{4}$ in.$\times\frac{5}{8}$ in., and with attached photomultiplier. The central crystal is about 9 in. from the target. The whole telescope may be rotated about an axis through the center of the target and perpendicular to the x-ray beam.

As is well known, stopped π^+ mesons disintegrate with a mean lifetime of 2.6×10^{-8} sec. The μ^+ mesons

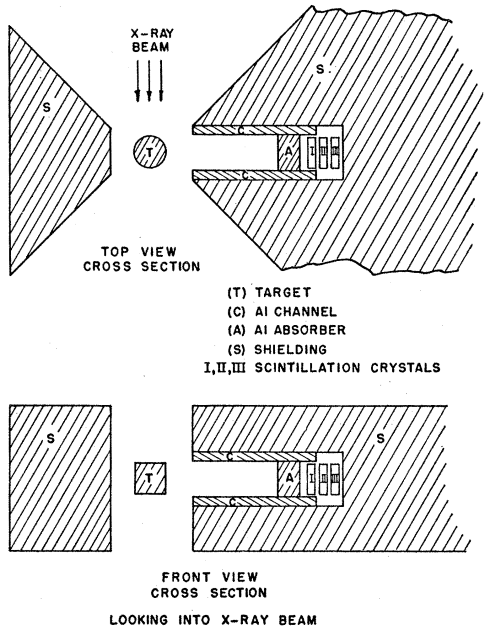

FIG. 5. Details of meson detector.

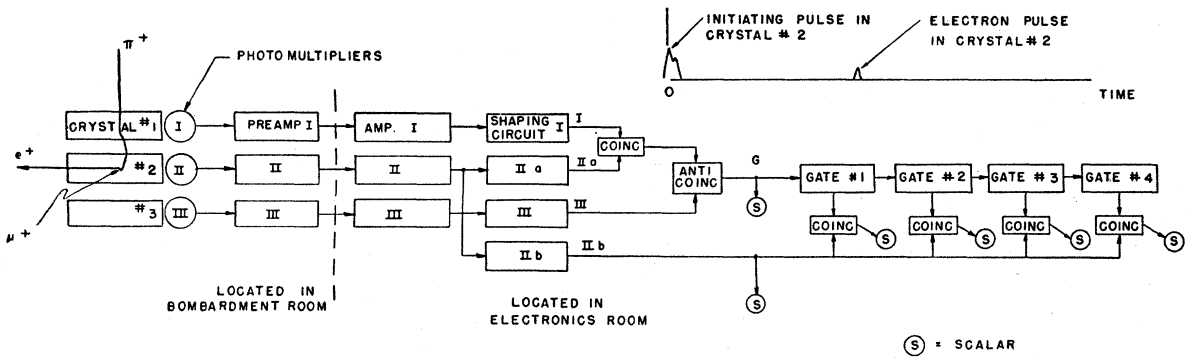

FIG. 6. Block diagram of electronics.

so produced disintegrate with a mean life of 2.2×10^{-6} sec, emitting positrons. On the other hand, π^- mesons coming to rest in condensed matter immediately form stars and have no delayed decay products. Our apparatus detects π^+, μ^+, and μ^- mesons, and does not distinguish between these. A particle is registered if it penetrates the aluminum absorber (Fig. 5), and crystal I, comes to rest in crystal II, and its decay electron appears within the time interval of one of several successive gates, each two microseconds long, initiated by the first event. A block diagram is shown in Fig. 6. Only standard electronic apparatus is required except, perhaps, for the discriminator in the decay electron pulse channel. This must have a short recovery time, since the decay electron pulse is always preceded by that of the stopping meson. For this purpose a biased positive feedback amplifier was used, with 5×10^{-7} sec recovery time, of a design by Wouters.

b. Accidental Counting Rate

Not all observed coincidences are due to time correlated events, but some, varying from between one and twenty percent of the counting rate in the first delay channel, are due to two uncorrelated events which have the proper time delay. The number of such events is calculated statistically as the product of the known single counting rates, resolving time, and reciprocal duty cycle. The quotient of resolving time and duty cycle is determined by testing the apparatus under conditions in which the number of time correlated events is small compared to the random events.

c. Experimental Checks on the Detection Method

Removal of the target, or of the liquid hydrogen from its container, resulted in a decrease in the meson counting rate by at least a factor of 100. Plateau characteristics (delay coincide rate as a function of minimum pulse height in a particular channel) are reproduced in Figs. 7, 8, and 9. They show that the pulses due to stopping mesons are rather uniform in height, but that those due to the decay electrons have a large spread. This is expected, since the decay electron ranges are large compared to crystal dimensions and the electrons leave the crystal in all directions with various path length. The shape of Fig. 10 has been checked theoretically.

The scintillation detectors are operated at the indicated pulse-height levels during all experiments. The levels are calibrated by means of a radium source. With the help of the plateau curves it is possible to calculate absolute cross sections, if it is assumed that the intercepts of the plateau curves with the abscissa corresponds to 100 percent detection efficiency. We estimate that the error in the absolute cross sections due to uncertainty in the detection efficiency is of the order of 10 percent. The differences in the absolute cross sections between previously reported results[2] and those of this paper are due to incorrect estimates of the decay electron detection efficiency before the experimental determination of Fig. 9.

The relative counting rates in the delay channels should reproduce the exponential $\mu\rightarrow e$ decay. This datum is obtained simultaneously with all measurements, some of it is shown in Fig. 10. Although statistically superior to previous measurements, they suffer from systematic error.[6] The lifetime determinations

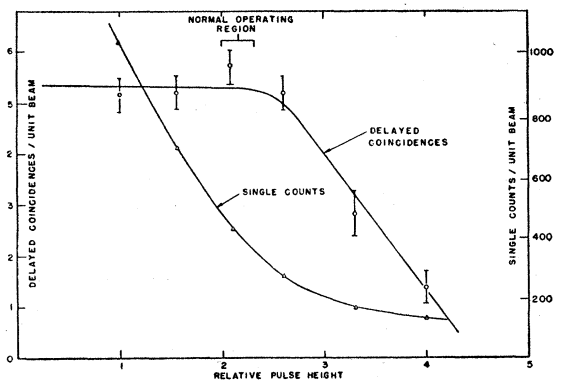

FIG. 7. Integral counting rates as a function of pulse height in crystal 1.

[6] This error is due to the fact that the pulse circuits do not trigger with uniform sensitivity for 1–2μ seconds after the initial (meson stopping) event. The decay electron is therefore not counted with the same efficiency in the first channel as in the others.

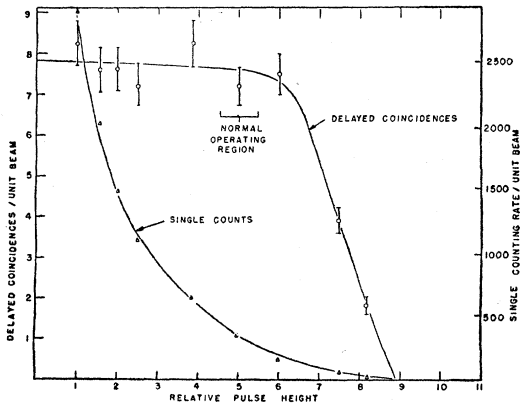

FIG. 8. Integral counting rates as a function of pulse height in channel II*a*.

serve as a check on the method, rather than as a better determination of the $\mu \rightarrow e$ decay constant.

In this connection it may be pointed out that although the apparatus detects π^+, μ^+, and μ^- mesons, all but 2–3 percent are π^+ mesons. μ^- mesons are produced at most in minute amounts, as shown by the experiments using photographic emulsion detectors.[1] The μ^- mesons which are counted are due to the 2–3 percent of the π^- mesons decaying in flight. Since both range and direction are approximately preserved in the decay, the chief effect is that besides the positive π-mesons, 2–3 percent of the negative pions are also counted. The hydrogen cross sections are not at all affected, since it is known from the work by Cook[7] in photographic emulsions that negative mesons are not produced by photons in hydrogen.

d. Angular and Energy Resolutions

The intensity of the x-ray beam limits the resolution which can be obtained without sacrificing statistical accuracy. In the geometry of Fig. 5, the detectors subtend a solid angle of approximately 0.03 sterad, an angular resolution of $\pm 7°$. The target thickness is 0.4 g/cm² in the liquid hydrogen experiments and 4 g/cm² in the subtraction experiments. The detector in which the meson stops is 2 g/cm² thick. The energy uncertainty which corresponds to this range uncertainty depends on the energy. For most of the spectrum it is approximately ± 3 Mev for the liquid hydrogen, and ± 5 Mev for the subtraction experiments. It is larger at low and smaller at high energies. Under these conditions the counting rate is approximately 10 mesons/min and a day's bombardment is required to obtain one point by subtraction with a statistical inaccuracy of 5 percent. Better angular resolution, and especially energy determination by magnetic analysis are difficult to achieve with present intensities.

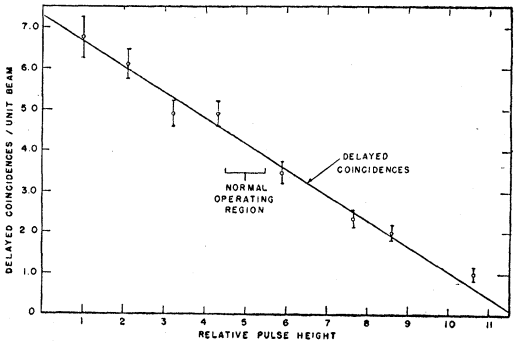

FIG. 9. Integral counting rate as a function of pulse height in channel II*b*.

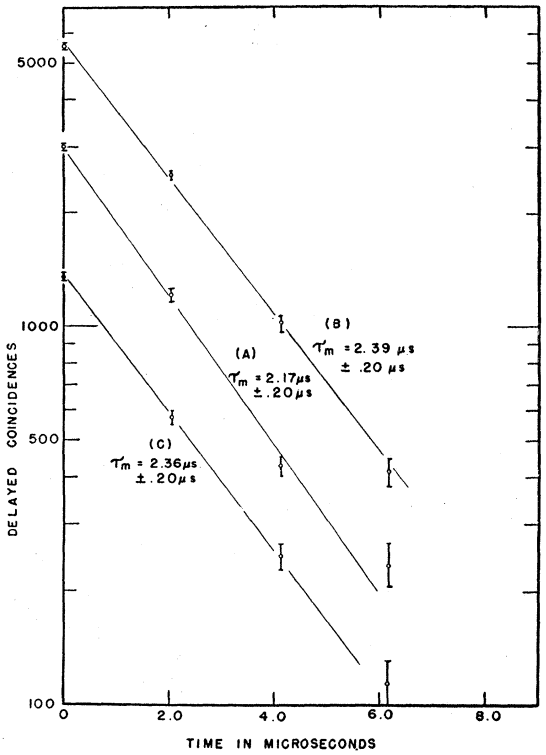

FIG. 10. Relative counting rate in the four delay channels for three sets of data.

e. Effects of Nuclear Interaction of Mesons

All methods of detecting mesons which depend on observing it at the end of its range suffer from the fact that the meson may be scattered or absorbed in nuclear collisions in the material which brings it to rest. The mean free path of 90-Mev mesons in aluminum, the absorbing material used in these experiments, has been measured and is 70 g/cm²[8] The data have been corrected for this absorption.

[7] L. J. Cook, to be published.

[8] Chedester, Isaacs, Sachs, and Steinberger, Phys. Rev. **82**, 958 (1951).

V. EXPERIMENTAL RESULTS

a. Energy Distribution of π^+ Mesons at 90° to the Beam Direction

The experiment was performed with carbon, paraffin, and liquid hydrogen targets. The geometry of the subtraction experiment is shown in Fig. 4. The targets are cylinders 2 in. high and 2 in. in diameter. The carbon target is laminated so that the ionization loss of the meson in the two targets is the same. The attenuation of the incident beam, chiefly due to pair creation, is 7 percent in the carbon, 5 percent in the paraffin target. The angular resolution is triangular, $\pm 10°$ at the base. The results are shown in Fig. 11.

Figure 12 represents the geometry, using a liquid hydrogen target. The target is designed and constructed by Cook. The energy resolution is ± 3 Mev and the angular resolution is triangular with $\pm 10°$ width at the base. Results are given in Fig. 13.

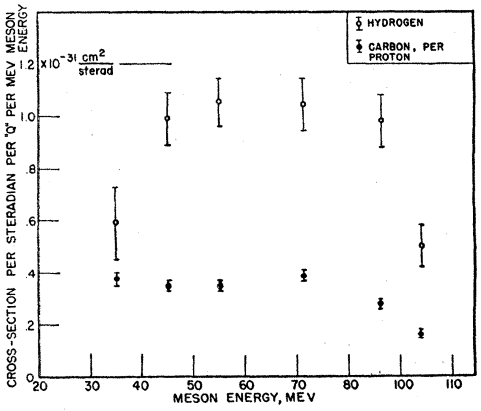

FIG. 11. Energy distribution of mesons produced at 90° by 325-Mev max energy x-rays on carbon and on hydrogen by subtraction.

As was pointed out in Sec. III, it is possible to derive the excitation function of the differential cross section from these data. Let the photon spectrum, $\phi(h\nu)$ be normalized so that

$$\int_0^{h\nu_{\max}} h\nu\phi(h\nu)dh\nu = h\nu_{\max} = 1\text{“}Q\text{”}.^9$$

Let $N(E)$ = number of mesons per unit meson energy per steradian per Q and per target atom. Then

$$d\sigma(h\nu)/d\Omega = [N(E)/\phi(h\nu)](dE/dh\nu),$$

where $h\nu$ and E are related [Eq. (1)] through the conservation laws.

The excitation function of the differential cross section for the production of π^+ mesons on hydrogen is shown in Fig. 14. Because of their superior statistical accuracy and energy resolution, only the liquid hydrogen results were used in the determination of the excitation function.

[9] The "Q" is a unit of x-ray flux. The number of Q's incident on a target is equal to the total incident x-ray energy divided by the maximum x-ray energy.

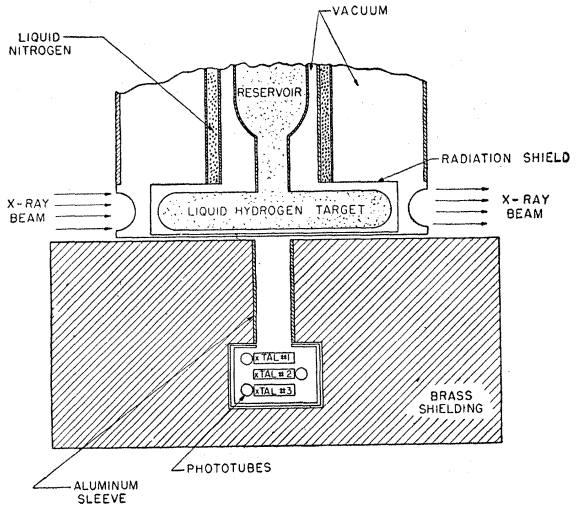

FIG. 12. Hydrogen target and geometry used in energy distribution measurements at 90°.

b. Angular Distribution

The angular distribution was also measured both by subtraction and with a liquid hydrogen target. At the various angles the meson range was chosen so that the responsible incident photons have the energy 255 Mev in the laboratory system, or 204 Mev in the center-of-mass system. The angular range was limited in the forward direction by an increasing accidental counting rate, and in the backward direction by the geometry of the apparatus. The liquid hydrogen target was designed by V. Peterseon and is shown in Fig. 15. The hydrogen is contained in an aluminum cup $1\frac{1}{2}$ in. in diameter, $1\frac{3}{4}$ in. high, and with 0.0015-in. wall thickness. The meson production in the walls of the cup is approxi-

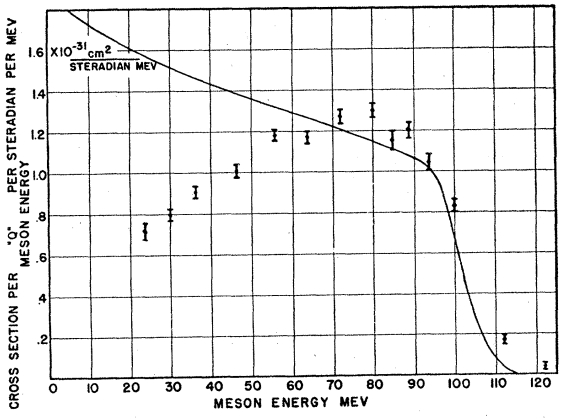

FIG. 13. Energy distribution of mesons produced by 325-Mev max energy x-rays on hydrogen, using liquid hydrogen target. Solid curve represents number of photons per unit meson energy. $\phi(h\nu)dh\nu/dE$. The derivative is calculated on the basis of formula (1).

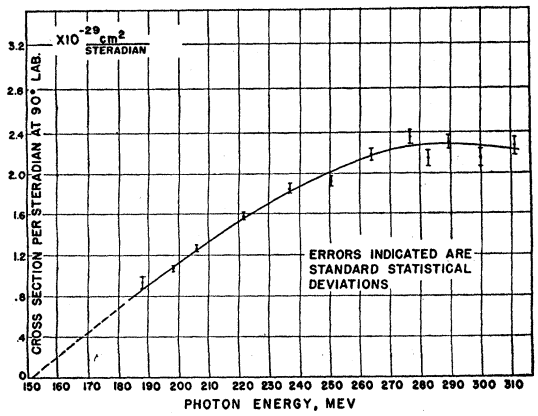

FIG. 14. Excitation function for the production of mesons by photons on hydrogen, at 90° to the beam.

mately 1 percent of that in hydrogen. The angular dispersion is triangular, ±6.5° at the base. Results are shown in Figs. 16 and 17.

c. Total Cross Section

Except for the missing experimental data at very large and very small production angles, the angular distribution data can be integrated to yield a total cross section. Twenty percent of the total solid angle lies in the unexplored region. Extrapolating the data linearly to small and large angles, we get a total cross section of $1.9\pm0.3\times10^{-28}$ cm² for the production of positive mesons on hydrogen by 255-Mev γ-rays.

VI. DISCUSSION OF RESULTS

We compare here briefly several theoretical suggestions with the experimental results. The photomeson production reaction provides a new domain for testing the theory of the interaction of the π-meson with nucleons, and it may be hoped that it will provide some new insight, and this because the reaction is particularly simple in the frame of the current approximate methods. The comparison need be made only for scalar and pseudoscalar mesons, since it is known that the pion has spin zero.[10]

The reaction has been studied theoretically from at least three points of view, which differ in the approximations used in the solution of the same equations of motion of the meson, nucleon, and electromagnetic fields.

1. Perturbation approximation.[11] It is assumed that the coupling of mesons and nucleons is weak, and the solution is the first term in an expansion in the coupling parameter. The higher order terms are increasingly difficult to evaluate. For the large known interaction of mesons and nucleons, the convergence is either slow or nonexistent. Pseudoscalar and pseudovector coupling of the pseudoscalar meson field to the nucleus give the

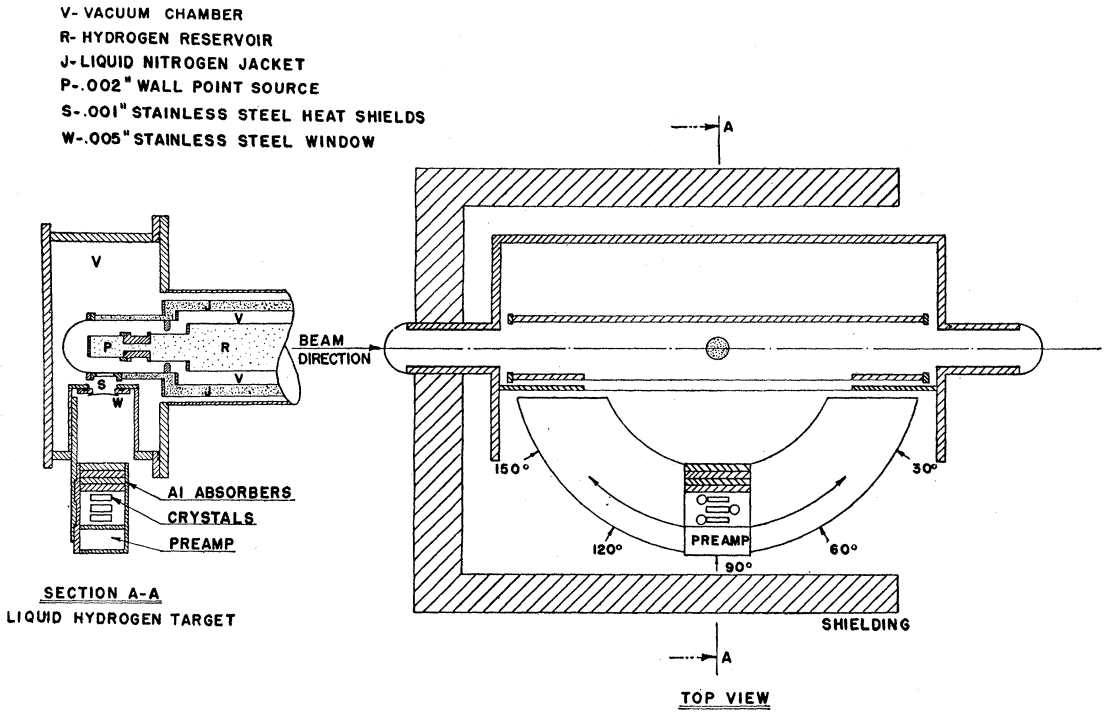

FIG. 15. Hydrogen target used in angular distribution measurements.

[10] Durbin, Loar, and Steinberger, Phys. Rev. **83**, 646 (1951); Clark, Roberts, and Wilson, Phys. Rev. **83**, 649 (1951).
[11] Perturbation theoretical results have been published by H. Feshbach and M. Lax, Phys. Rev. **76**, 134 (1949); K. A. Brueckner, Phys. Rev. **79**, 641 (1950); G. Araki, Prog. Theor. Phys. **5**, 507 (1950).

same result in the first order. The pseudovector coupling theory diverges in higher order.

2. Strong coupling or classical approximation, in the strong coupling theory[12] it is assumed that the coupling parameter is large; in the classical approximation[13] the meson field is not quantized, but the strength of the coupling is arbitrary. These approximations are equivalent and give the same results. In order to permit a solution of the equations, it must be further assumed that the nucleons are infinitely heavy (neglect of recoil) and it is necessary to introduce an effective nuclear radius of the order of the nucleon Compton wavelength to allow the convergence of certain integrals.

3. In the Tomonaga intermediate coupling approximation[14] the field equations are integrated in successive steps; the first corresponds to no mesons in the self field of the nucleon, the second to one meson, and so on. The approximations involve chiefly the choice of the approximate solutions for the meson field wave functions, as well as neglect of nuclear recoil. Because of the nonrelativistic approximations (nuclear recoil neglect), the classical (strong coupling) and Tomonaga calculations are possible only in pseudovector coupling in the case of pseudoscalar mesons.

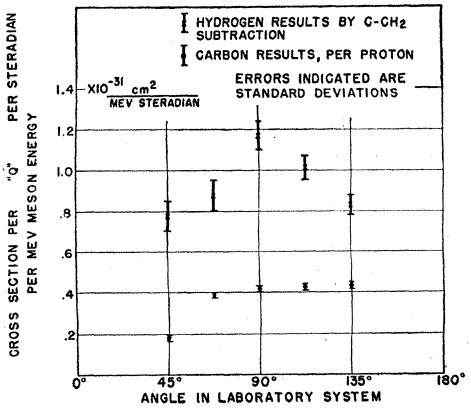

FIG. 16. The production of mesons on carbon and on hydrogen by subtraction, at five angles. The meson energies are 48 Mev at 135°, 57 Mev at 112.5°, 67 Mev at 90°, 82 Mev at 67.5°, and 96 Mev at 135°, chosen so that the responsible photon energy in the free proton collision is 255 Mev.

Except for minor relativistic corrections present only in the perturbation theory, all three approximations give the same results. These are

$$\frac{d\sigma}{d\Omega}=\frac{1}{4}\frac{g^2}{4\pi}\frac{k^2\sin^2\theta}{E^2h\nu^2(1-v\cos\theta)^2}\times\text{const (scalar)}, \quad (2)$$

$$\frac{d\sigma}{d\Omega}=\frac{f^2}{4\pi}\frac{k^2}{\kappa^2h\nu^2}\left[1-\frac{\kappa^2k^2\sin^2\theta}{2E^2h\nu^2(1-v\cos\theta)^2}\right]\times\text{const (pseudoscalar)}, \quad (3)$$

where $\hbar=c=1$; $\alpha=1/137$; E, k = meson energy, momentum; $h\nu$ = photon energy; v = meson velocity; θ = production angle of meson with respect to photon; g, f = coupling constants in scalar and pseudoscalar theory (pseudovector coupling). In pseudoscalar coupling f should be replaced by $\kappa g/2M$.

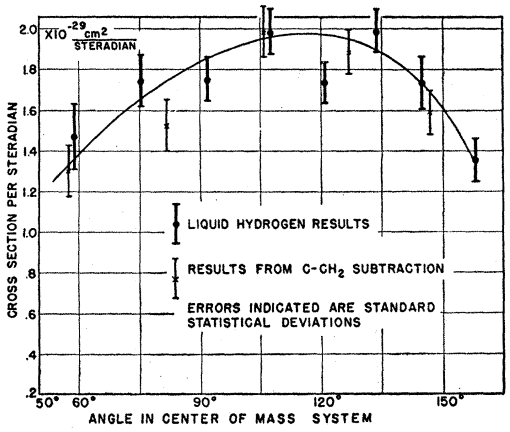

FIG. 17. Angular distribution for the production of mesons by photons on hydrogen. The meson energies are as in Fig. 16.

The constant is unity in the weak coupling (perturbation) limit, and has been evaluated by Watson and Hart[14] in the transition region of weak to strong coupling. In the limit of strong coupling the constant is $\frac{1}{4}$ in the scalar theory, and $\frac{1}{6}$ in the pseudoscalar theory. In Fig. 18 Watson and Hart's results are reproduced for the pseudoscalar theory in the transition region from weak to strong coupling. The relativistic perturbation result[15] is compared with the experiment in Figs. 19 and 20. The angular distribution in the scalar theory has a dipole character and is peaked at small angles because of the retardation factor $(1-v\cos\theta)^{-2}$. In

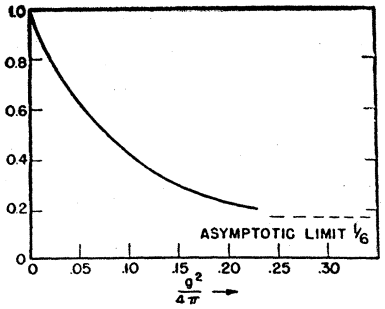

FIG. 18. The ratio of photomeson production in the Tomonaga approximation to its value in the weak coupling approximation (after Watson and Hart).

[12] Y. Fujimoto and H. Miyazawa, Prog. Theor. Phys. 5, 1052 (1950).

[13] K. A. Brueckner and K. M. Case, to be published. Also H. W. Lewis, private communication.

[14] K. M. Watson and E. W. Hart, Phys. Rev. 79, 918 (1950).

[15] The result in perturbation theory is:

$$\frac{d\sigma}{d\Omega}=\frac{\alpha}{4}\frac{g^2}{4\pi}\frac{k\left\{\dfrac{k^2\sin^2\theta(\pm M-\mathbf{p}\cdot\mathbf{p}_0)}{E^2h\nu^2(1-v\cos\theta)^2}-\dfrac{k^2\sin^2\theta]}{(1-v\cos\theta)Eh\nu}+\dfrac{\mathbf{p}\cdot h\boldsymbol{\nu}}{\mathbf{p}_0\cdot h\boldsymbol{\nu}}\right\}}{h\nu E_NE_p[1+E/M-(h\nu-p_0)E\cos\theta/kM](1+p_0/E_p)}$$

where the + and − signs refer to scalar and pseudoscalar theory respectively. $\mathbf{A}\cdot\mathbf{B}$ are four-vector products. $\mathbf{p}_0$ and $\mathbf{p}$ are energy-momentum vectors of incoming and outgoing nucleons, respectively.

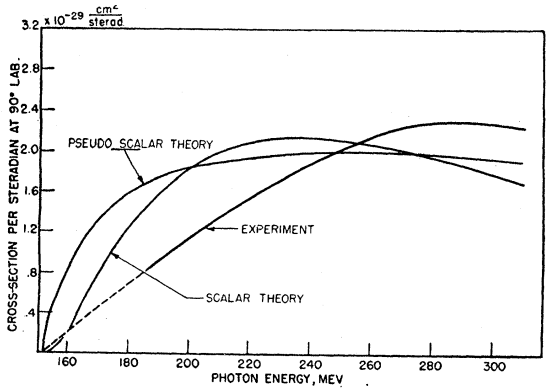

FIG. 19. Energy distribution in the perturbation theory, compared with the experimental result.

pseudoscalar theory there is also the dipole term, but the predominant term involves a change of the nucleon spin, and is isotropic. The two interfere destructively. The excitation function differs chiefly in that the scalar theory starts at threshold as $(h\nu-h\nu_0)^{\frac{1}{2}}$ and the pseudoscalar theory more steeply as $(h\nu-h\nu)_0^{\frac{1}{2}}$. Neither theory gives good experimental agreement at low meson energies in the excitation function. The energy dependence of the matrix element in pseudoscalar theory is very small, so that the pseudoscalar result in Fig. 19 is almost entirely kinematical. Comparison with the experimental results shows that the square of the matrix element actually increases with energy by a factor of approximately two in the observed energy range.

In the angular distribution, the pseudoscalar theory is in fair agreement with the experimental result, although the experimental points fall considerably below the theoretical at backward angles. The scalar results are, however, in violent disagreement. We wish to argue, that since the theoretical result is independent of the approximation used, and actually follows directly from the spin independent isotropic meson-nucleon interaction, it is sufficiently firm to rule out the possibility that the charged pion is scalar, on the basis of these experiments. This is in agreement with the conclusion of Brueckner, Serber, and Watson[16] on the basis of the experiments of Panofsky *et al.*[17] on the absorption of π-mesons in deuterium.

The photomeson production is well suited for a determination of the coupling constant in the meson nucleon interaction, since the pseudoscalar theory is in fair agreement with the experiment. The pseudovector coupling constant which gives best agreement with the angular distribution at 255-Mev photon energy is $f^2/4\pi=0.37$ in the relativistic weak coupling limit.[15] The nonrelativistic weak coupling result (Eq. (3)) requires $f^2/4\pi=0.16$. However, it may be seen from the result of Watson and Hart, Fig. 18, that this is much too high for the validity of the weak coupling approximation, and that the approximation of strong coupling is more nearly valid. The value of the coupling constant to be used in theories which do not assume its smallness must then be six times greater, or $f^2/4\pi=1.0$, in order to maintain agreement with this experiment. The inadequacies of the theory, however, prevent one from attaching significance to the exact result.

We turn to a discussion of photomeson production in a complex nucleus. Experimentally we see that the differential cross section per proton in carbon is lower than the elementary process by a factor five at 45°, and by a a factor two at 135°. The mean energy of the mesons produced in carbon is approximately 3.5 Mev lower than that in hydrogen, at 90° in the laboratory system and integrated over the continuous spectrum of the meson beam.

The additional nucleons act in two ways: (1) They interfere in the creation of the meson. (2) They may reabsorb the meson before it escapes. Effect 1 is discussed by Feshbach and Lax[18] and by Chew and Lewis.[19] The latter treats specifically the deuteron, but the arguments can be extended to more complex nuclei. It is shown, especially by Chew and Lewis, that the chief effect in the complex nucleus is the exclusion principle interference in the final state, which reduces the cross section for those states, in which the nucleons have small total momentum in the final state. This reduces markedly the production of mesons in the forward directions, because the momentum transfer to the nuclear system is then small. It has also the effect of raising the average energy left to the nuclear system, and therefore reducing the average energy of the meson, as observed. The reduction in cross section is given by a form factor

$$\sigma=\sigma_0[1-F(D)]; \quad F(D)\simeq\int\psi^2\exp(i\mathbf{D}\cdot\mathbf{r})d\mathbf{r};$$

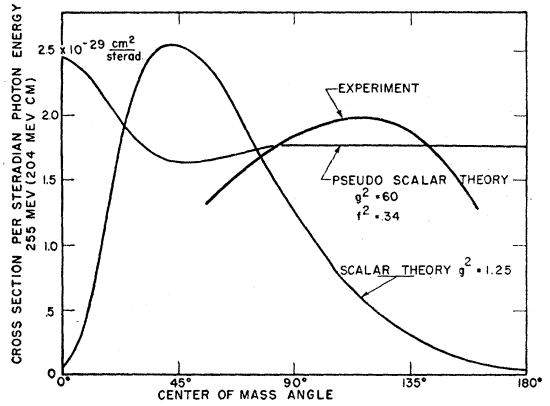

FIG. 20. Angular distribution of photomesons (photon energy 255 Mev) in the perturbation theory, compared with the experimental result.

[16] Brueckner, Serber, and Watson, Phys. Rev. **81**, 575 (1951).
[17] W. K. H. Panofsky, Phys. Rev. **81**, 565 (1951).
[18] H. Feshbach and M. Lax, Phys. Rev. **76**, 134 (1949).
[19] G. Chew and H. W. Lewis, Phys. Rev. **84**, 779 (1951).

where σ_0 = differential cross section for the elementary act; σ = differential cross section in carbon, per proton; $\mathbf{D}$ = total momentum of final nuclear system; ψ = wave function of protons in a carbon nucleus.

The simplicity of the form factor is due to a closure approximation.[19] The relation (1) is a good approximation for nuclei larger than helium. In the case of deuterium the connection is more complicated. It depends on the form of the meson-nucleon interaction, specifically, on whether or not the spin state of the nucleon changes in the process of meson emission. In the case of heavier nuclei, the Pauli interference does not depend on a possible spin change. To compare with the experiment, we need to know ψ. We use the wave function empirically determined by Chew and Goldberger[20] in an analysis of the deuteron pick-up reaction

$$\psi=(\alpha_p^3/\pi)^{\frac{1}{2}}e^{-\alpha_p r};\quad \alpha_p=1.3(\kappa c/\hbar).$$

Then

$$F(D)=\alpha_p^4/(\alpha_p^2+\tfrac{1}{4}D^2)^2.$$

It is also necessary to know the correspondence between the nuclear recoil D and the meson production momentum k, which is observed experimentally. There is no one-to-one correspondence between these quantities, except in the elementary process. However, as Chew and Lewis[19] point out, the average nuclear recoil D will be approximately equal to the corresponding recoil momentum in the case of photoproduction in hydrogen. With these assumptions it is possible to make the comparison between the theoretical and experimental results, shown in Fig. 21. The solid line shows the effect of the Pauli principle alone. The absorption mean free path for mesons of this energy is approximately 4×10^{-13} cm,[21] so that about 50 percent of the mesons produced in carbon should be reabsorbed. This correction brings the theoretical expectation below the experimental points (dotted curves, Fig. 22).[13] The theory is in agreement with the observed angular distribution, and although it overestimates the interference effect slightly, the basic assumptions are confirmed.

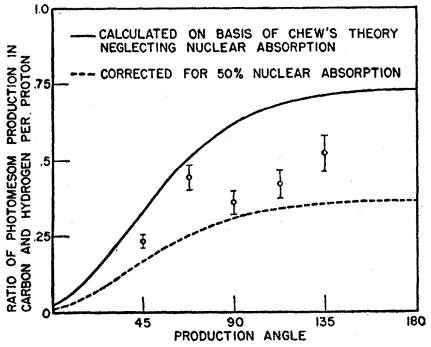

FIG. 21. Experimental and theoretical ratio of the photomeson production cross section in carbon, per proton, with respect to hydrogen.

We wish to thank Professor E. B. McMillan for the use of the synchrotron, and for his kind assistance during the course of the experiments. We are indebted to Dr. L. Cook and Dr. V. Peterson for the use of liquid hydrogen targets, and to Dr. W. Blocker and Dr. R. Kenney for the absolute calibration of the beam monitor. The bombardments were made by the operating crew of the Berkeley synchrotron under the direction of W. Gibbins and J. McFarlane.

[20] G. Chew and M. Goldberger, Phys. Rev. **77**, 470 (1950).

[21] Byfield, Lederman, and Kessler, unpublished; Isaacs, Sachs, and Steinberger, unpublished.